Running head: Developmental Roles of Rice EJC Core

Corresponding author: Chaoying He State Key Laboratory of Systematic and Evolutionary Botany Institute of Botany, Chinese Academy of Sciences Nanxincun 20, Xiangshan, Haidian 100093 Beijing, China; E-mail: <u>chaoying@ibcas.ac.cn</u> Tel: +86-10-62836085 Fax: +86-10-62590843.

Research Area: Genes, Development and Evolution

Downloaded from www.plantphysiol.org on May 12, 2014 - Published by www.plant.org Copyright © 2014 American Society of Plant Biologists. All rights reserved. **Copyright 2014 by the American Society of Plant Biologists**

Research Article

Uncovering Divergence of Rice EJC Core Heterodimer Gene Duplication Reveals Their Essential role in Growth, Development and Reproduction¹

Pichang Gong^{a,b}, and Chaoying He^{a,2}

a State Key Laboratory of Systematic and Evolutionary Botany, Institute of Botany, Chinese Academy of Sciences, Nanxincun 20, Xiangshan, Haidian, 100093 Beijing, China;

b University of Chinese Academy of Sciences, Yuquan Road 19, 100049 Beijing, China.

For correspondence: E-mail: <u>chaoying@ibcas.ac.cn</u>; Tel: +86-10-62836085; Fax: +86-10-62590843.

One-Sentence Summary:

Divergence of each EJC core subunit paralog and the MAGO-Y14 heterodimer duplicates in rice implicates the importance of these genes in cereal growth, development, reproduction and adaptive evolution.

Footnotes:

1 This work was supported by a grant (2009ZX08009-011B) from the Chinese Ministry of Agriculture Transgenic Major Project and by a grant (31370259) from the National Natural Science Foundation of China.

2 For correspondence, E-mail: <u>chaoying@ibcas.ac.cn</u>; Tel: +86-10-62836085; Fax: +86-10-62590843.

Abstract

The exon junction complex (EJC) plays important developmental roles in animals; however, its role in plants is not well known. Here, we show various aspects of divergence of each duplicated MAGO- and Y14-gene pair in rice encoding the putative EJC core subunits that form the obligate MAGO-Y14 heterodimers. OsMAGO1, OsMAGO2 and OsY14a were constitutively expressed in all tissues while OsY14b was predominantly expressed in embryonic tissues. OsMAGO2 and OsY14b were more sensitive to different stresses than OsMAGO1 and OsY14a, and their encoded protein pair shared 93.8% and 46.9% sequence identity, respectively. Single MAGO downregulation in rice did not lead to any phenotypic variation; however, double-gene knockdowns generated short rice plants with abnormal flowers, and the stamens of these flowers showed inhibited degradation and absorption of both endothecium and tapetum, suggesting that OsMAGO1 and OsMAGO2 were functionally redundant. OsY14a knockdowns phenocopied OsMAGO1OsMAGO2 mutants while downregulation of OsY14b failed to induce plantlets, suggesting the functional specialization of OsY14b in embryogenesis. OsMAGO10sMAGO20sY14a triple downregulation enhanced the phenotypes of OsMAGO10sMAGO2 and OsY14a downregulated mutants, indicating that they exert developmental roles in the MAGO-Y14 heterodimerization mode. Modified gene expression was noted in the altered developmental pathways in these knockdowns, and the transcript splicing of OsUDT1, a key regulator in stamen development was uniquely abnormal. Concomitantly, MAGO and Y14 selectively bound to the *OsUDT1* pre-mRNA, suggesting that rice EJC subunits regulate splicing. Our work provides novel insights into the function of the EJC locus in growth, development and reproduction in angiosperms, and suggests a role for these genes in the adaptive evolution of cereals.

Keywords: exon junction complex (EJC); MAGO-Y14 heterodimer; splicing; male fertility; embryogenesis; rice

INTRODUCTION

The exon junction complex (EJC) is one of the fundamental machineries in the post-splicing processes in eukaryotes (Tange et al., 2004). The complex includes over ten different proteins, such as MAGO (MAGO NASHI), Y14 (Tsunagi or RBM8), eIF4A-III and BTZ (Barentsz, also MLN51) (Kim et al., 2001; Le Hir et al., 2001; Mohr et al., 2001; Palacios et al., 2004; Park et al., 2009; Zhao et al., 2000). MAGO and Y14 are core subunits of the EJC (Kataoka et al., 2001; Le Hir et al., 2001). Both subunits have been confirmed to direct normal development of animals. In Drosophila *spp.*, a single point mutation in the *MAGO* locus causes several developmental defects, such as improper development of the posterior lobe of the embryo, non-viable egg sacs in female offspring, and impairment of germ plasm cell polarity and germline stem cell differentiation (Boswell et al., 1991; Micklem et al., 1997; Newmark and Boswell, 1994; Newmark et al., 1997; Parma et al., 2007). In *Caenorhabditis elegans*, the *mag-1* gene is involved in hermaphrodite germ-line sex determination (Li et al., 2000). In mouse, *MAGO* gene is related to cell cycle regulation (Inaki et al., 2011). Tsunagi, the Y14 ortholog (Kataoka et al., 2000), is involved in embryogenesis and germline sexual switching (Kawano et al., 2004) and regulating oocyte specification (Lewandowski et al., 2010; Parma et al., 2007). MAGO and Y14 have been recently shown to be involved in the eye development of *Drosophila ssp.* (Ashton-Beaucage et al., 2010; Roignant and Treisman, 2010). MAGO regulates proliferation and expansion of neural crest-derived melanocytes (Silver et al., 2013), whereas Y14 targets neuronal genes to regulate anxiety behaviors in mice (Alachkar et al., 2013). Therefore, these studies confirm the role of MAGO and Y14 genes in multiple related developmental roles "in animal species." However, limited evidence for the developmental role of these genes is found in plants. PFMAGO proteins (MAGO homologs from *Physalis floridana*) via interacting with the MADS-domain protein MPF2 (MADS protein2 from *P. floridana*) are responsible for male fertility (He et al., 2007). Arabidopsis thaliana AtMago gene is required for pollen grain development and its knockout is lethal (Johnson et al., 2004; Park et al., 2009). Mutation of *Mv-mago* disrupts spermatogenesis in *Marsilea vestita* (Boothby and Wolniak, 2011;

van der Weele et al., 2007). Besides, plant *MAGO* genes also seem to have broad roles in the growth and development of other plant organs. Downregulating *AtMago* affects the development of root, shoot, floral meristem and seed (Park et al., 2009). *TcMago* is preferentially expressed in root hairs in *Taiwania cryptomerioides* and overexpressing this gene produces taller transgenic tobacco plants with increased root hairs (Chen et al., 2007). While the knockdowns of *AtY14* yield a lethal phenotype (Park et al., 2009).

MAGO and Y14 proteins form obligate heterodimers (Shi and Xu, 2003; Gong et al., 2014) in eukaryotes. However, only MAGO-Y14 heterodimer in metazoans binds to the mRNAs 20-24 nucleotides upstream of the exon-exon junctions affecting the multiple steps of post-splicing processes, such as mRNA intracellular export, cytoplasmic localization, nonsense-mediated mRNA decay (NMD), and translational enhancement (Hachet and Ephrussi, 2001; Lee et al., 2009; Tange et al., 2004). These subunits were recently demonstrated to be specifically involved in the splicing process of genes with large introns and heterochromatin localization in Drosophila ssp. (Ashton-Beaucage et al., 2010; Roignant and Treisman, 2010). The regulation of plant development by EJC is poorly understood. Furthermore, the retention of two copies for each gene family in cereals (Gong et al., 2014), suggests a specific evolutionary role of these genes in cereal evolution. In the present study, we characterized OsMAGO1, OsMAGO2, OsY14a and OsY14b in rice to address the developmental role of EJC subunits in plants. Our study showed the divergence of each paralogous gene pair, and that they are essential to both vegetative and reproductive development. The transcript splicing of the rice undeveloped tapetum 1 (OsUDT1), a major regulator of the early tapetum development (Jung et al., 2005), was found to be specifically affected by depletion of these EJC subunits in rice. Our data provide the first insight into the essential role of the EJC in growth, development and reproduction of rice with an implication of adaptive evolution in cereals.

RESULTS

Divergence in Expressions and Sequences of Rice MAGO and Y14 Paralogs

6

Using qRT-PCR, we showed that, during normal development of rice, the genes, OsMAGO1 and OsMAGO2, OsY14a were constitutively expressed in callus, all tissues of seedlings, floral organs and seeds (Figure 1). The difference in expression of these genes was not significant, suggesting co-regulation of their expression in rice development. However, OsY14b had a different expression pattern and was expressed in callus, early developmental stage of seed germination and floral tissues, but not in seedlings (Figure 1). Thus, OsY14b may have a specialized role in rice development. The expression of OsMAGO1 and OsY14a was studied in response to various stimuli. We observed that the *OsMAGO2* expression was significantly ($p \le 0.001$) induced by brassinolide (BR), abscisic acid (ABA), gibberellic acid 3 (GA3), and indole acetic acid (IAA) while OsY14b expression was significantly (p < 0.001) induced by BR, GA3, ABA and IAA (Figure S1A-D). OsY14b was also significantly influenced (p < 10.01) by high temperature, salinity stress and water deficiency (Figure S1E-H). Therefore, the mRNA expression of *OsMAGO2* and *OsY14b* is more sensitive to various external stimuli as compared to that of OsMAGO1 and OsY14a. Furthermore, OsMAGO1 and OsMAGO2 shared 93.8% sequence identity while OsY14a and OsY14b shared 46.9% identity (Gong et al., 2014). Thus, relative rapid divergence of rice Y14 might drive the functional divergence of the MAGO-Y14 dimers, and OsY14b might be under a neo- or subfunctionalization process.

Subcellular Localization and Heterodimerization of Rice MAGO and Y14

The open reading frames (ORFs) of rice *MAGO* and *Y14* were fused in-frame with green fluorescence protein gene (GFP) and were transiently expressed in plant cells to prove that sequence divergence may alter the subcellular localization of a protein. We found that OsMAGO1, OsMAGO2 and OsY14b showed identical distribution in cells, and were localized in the nuclei and cytoplasm (Figure 2A, B and D), similar to their homologs in other reported species. Surprisingly, OsY14a seemed to be uniquely localized in the nuclei (Figure 2C) deviating from the established subcellular localization of these EJC subunits. GFP alone, as the control, was expressed in both nuclei and cytoplasm (Figure 2E). These, again, reflect a more rapid divergence of

rice Y14- than MAGO-pair after duplication.

Rice MAGO and Y14 formed heterodimers in yeast (Figure S2A and B; Gong et al., 2014). The present study used bimolecular fluorescence complementation analyses (BiFC) in plant cells to study this heterodimerization. The yellow fluorescence protein (YFP) was divided into N-terminal (YN) and C-terminal (YC) halves. The ORFs of these genes were separately fused with either YN or YC and co-expressed. Fluorescence was observed when two proteins fused to each YFP half interacted with one another. A YFP signal was detected when fusion proteins YC-OsMAGO1 (or 2) and YN-OsY14a (or b) were co-expressed (Figure 2F-I). In contrast, no YFP signal was observed when fusion proteins YC-OsY14a and YN were used as controls (Figure 2J). In line with subcellular localization pattern of rice Y14 proteins, the interaction signal of OsMAGO1 (or 2) with OsY14a was observed in the nuclei only, whereas their interactions with OsY14b occurred in both nuclei and cytoplasm. Nonetheless, OsMAGO1 preferentially interacted with OsY14a while OsMAGO2 heterodimerized with OsY14b (p < 0.01; Figure S2C and D), indicating a potential functional separation between OsMAGO1-OsY14a and OsMAGO2-OsY14b.

The above revealed divergence may cause a functional divergence in each paralogous gene pair in rice. The developmental role of these EJC genes was further characterized using RNA interference (RNAi). Table S1 and Table S2 detail the independent transgenic lines that were generated and characterized for RNAi.

OsY14a Is Essential for Rice Growth, Development and Reproduction

Seven independent *Ubi:OsY14a*-RNAi transgenic lines (YaL1-YaL7) were analyzed, and six of them showed significant downregulation of *OsY14a* mRNA while mRNA of *OsY14b*, *OsMAGO1* and *OsMAGO2* were not affected (Figure S3A). The six *OsY14a* knockdowns showed similar phenotypic variations (Table S2) but were significantly different from the wild-type (WT). The transgenic plants at the heading stage were dwarfed in height as compared to WT (Figure 3A). In mature plants, the wild-type had five internodes in total which were named I to V from the top to the

bottom (Figure 3B). The panicle length (YaL4, 13.23 ± 0.13 cm; WT, 22.07 ± 0.26 cm; p < 0.001) and the culm length (YaL4, 49.32 ± 0.21 cm; WT, 82.90 ± 0.56 cm; p < 0.001) 0.001) of *Ubi:OsY14a*-RNAi transgenic plants were significantly shorter as compared to WT (Figure 3B and C). The decreased culm length was mainly due to the reduced length of each internode. In particular, internode 'V' was absent in the OsY14a downregulated transgenic plants. Furthermore, in comparison to WT (Figure 3D and H), the florets developed bigger lemma and palea (Figure 3E and I; Table S2). Furthermore, the epidermal cells on the lemma were significantly longer than the wild-type (Figure 3F and G; Figure S4A). The female organs were fertile since they could produce normal seeds when crossed with the wild-type pollen (Figure 3J and K; Table S3). However, the stamen and its filament became pale and were shorter than those in the WT (Figure 3L and M; Table S2). Cell size on the filament and stamen became significantly smaller than wild-type (Figure 3N-Q; Figure S4B and C) and resulted in reduced stamen and filament size. Pollen maturation was inhibited in the transgenic plants as compared to WT (Table S2). A substantial proportion of pollen grains in the transgenic plants (Figure 3S) were not stained dark blue using the iodine-potassium (I_2 -KI) staining method as compared to the wild type (Figure 3R) further proving that pollen maturation was inhibited in the RNAi lines. Germination pole was normal, but pollen morphology was abnormal (Figure 3T-Y). YaL7 without affecting OsY14a expression had no phenotypic defect (Figure S3A; Table S2).

OsY14b Is Required in Rice Embryonic Organogenesis and Development

Surprisingly, transgenic plants could not be regenerated from *Ubi:OsY14b*-RNAi lines with extra effort (Table S1). The callus formation was normal (Figure S5A), and tiny shoot-like structures were sometimes regenerated (Figure S5B). However, they were not able to develop into plantlets and finally withered and died (Figure S5C). These observations suggest that *OsY14b* is essential in shoot formation from the callus and in early shoot development as evident from gene expression analyses (Figure 1). Five independent calli with tiny green shoots were examined and were found to have extremely low levels of *OsY14b* expression, whereas the expression levels of *OsY14a*,

OsMAGO1 and *OsMAGO2* were not affected (Figure S5D). The failure in plant regeneration of *OsY14b*-RNAi suggested that downregulation of this gene was lethal to the growth and developments of rice plants.

Two MAGO Genes Play a Redundant Role in Rice Growth and Development

The 3'untranslated region (3'UTR) of OsMAGO1 was first used to silence OsMAGO1 gene in rice (Table S1). Five of six Ubi:OsMAGO1-3'UTR-RNAi transgenic plants (M1L1-M1L6) were associated with severe and specific downregulation of OsMAGO1 (Figure S3B). However, they did not produce any phenotypic variations in comparison with wild-type (Figure S6; Table S2) indicating a potential functional redundancy between OsMAGO1 and OsMAGO2. Therefore, we tried to use their coding regions (CDS) to silence the two genes simultaneously (Table S1). Altogether we characterized 13 independent transgenic rice lines for Ubi:OsMAGO1-CDS-RNAi (5 lines) and Ubi:OsMAGO2-CDS-RNAi (8 lines). Three lines (M2L1-M2L3) with severely downregulated OsMAGO2 were identified in Ubi:OsMAGO2-CDS-RNAi transgenic plants (Figure S3D). The phenotypes of these three plants were not different from wild-type (Table S2). However, six lines with severe and specific downregulation of both OsMAGO1 and OsMAGO2 were further obtained from Ubi:OsMAGO1-CDS-RNAi (M1L7-M1L9) and Ubi:OsMAGO2-CDS-RNAi (M2L4-M2L6) (Figure S3C and D). These transgenic plants showed dramatic phenotypic variations (Table S2). These transgenic plants at heading stage were smaller in size than wild-type. At the maturation stage, the panicle length (M1L7, 15.30 ± 0.14 cm; M2L6, 14.07 ± 0.20 cm; WT, 22.07 ± 0.26 cm; p < 0.001) and culm $(M1L7, 54.67 \pm 0.32 \text{ cm}; M2L6, 48.38 \pm 0.24 \text{ cm}; WT, 82.90 \pm 0.56 \text{ cm}; p < 0.001)$ of these transgenic plants were significantly shorter in comparison with wild-type (Figure 4A and B). The decreased culm length can be attributed to the reduced length of each internode; especially the I internode. Furthermore, these transgenic plants lacked the V internode (Figure 4A and B). Compared with wild-type (Figure 4C), the florets were bigger in the RNAi lines (Figure 4D and E). The increased lemma resulted from an increase in cell expansion (Figure 4F-H; Figure S4A). The female

organs looked normal and were fertile (Figure 4I-K; Table S3), while the stamen and its filament became significantly shorter than wild-type. Unlike the WT (Figure 4L), one filament bearing two stamens often developed in these transgenic plants (Figure 4M and N; Table S2). Cells on The stamen and filament became smaller as compared to the WT (Figure 4O-T; Figure S4B and C). A substantial proportion of pollen grains were not only immature as revealed by I₂-KI staining (p < 0.001; Figure 4U-W; Table S2) but were also deformed (Figure 4X-Z). The two rice *MAGO* genes are; therefore, functionally redundant.

OsMAGO1OsMAGO2 double knockdowns showed similar phenotypic variations as observed in *Ubi:OsY14*a-RNAi plants, suggesting that these genes may exert their roles through the MAGO-Y14 heterodimers.

Rice MAGO and Y14 Exert Their Roles in an Obligate Heterodimerization Mode In order to evaluate the developmental roles of the MAGO-Y14 heterodimers, we generated OsMAGO1OsMAGO2OsY14a knockdowns (OsY14b was excluded due to the lethality of single knockdowns) using the Ubi:OsMAGO1-CDS-OsY14a construct. Seven rice RNAi lines (MYaL1-MYaL7) were analyzed, and six of them showed a strong downregulation of OsMAGO1, OsMAGO2 and OsY14a (Figure 5A). These triple gene knockdowns featured similar phenotypic variation as observed in the knockdowns of either double OsMAGO1OsMAGO2 or single OsY14a. The transgenic plants were smaller in size than the wild-type (Figure 5B). Panicle lengths (MYaL2, 11.23 ± 0.11 cm; WT, 22.07 ± 0.26 cm; p < 0.001) and culm lengths (MYaL2, 43.90 \pm 0.23 cm; WT, 82.90 \pm 0.56 cm; p < 0.001) of these transgenic plants were significantly shorter than the WT (Figure 5C and D). The decreased culm length can again be attributed to the reduced length of each internode. The V internode was also absent in these transgenic plants (Figure 5C and D). Compared to the wild-type, the floret developed bigger lemma and palea (Figure 5E and F; Table S2) with bigger cells (Figure 5G and H; Figure S4A). The female organs were normal (Figure 7K and L; Table S3), whereas the stamen and its filament became pale and shorter as compared to those in wild-type (Figure 5M and N; Table S2) with smaller cells

(Figure 5O-R; Figure S4B and C), suggesting a functional abnormality. A large portion of pollen grains was immature (p < 0.001; Figure 5S-T; Table S2) and deformed (Figure 5U and V). These findings verify that both rice *MAGO* and *OsY14a* have important roles through heterodimerization in the same developmental pathways. The essential role in male fertility was particularly investigated.

Downregulating MAGO or Y14 Causes Abnormal Pollen Development in Rice

RNAi transgenic plants showed a decreased seed setting rate once MAGO and Y14 genes were downregulated (Table S2). However, their seed-setting rate was similar to that of artificially pollinated wild-type plants when crossed with wild-type pollens (Table S3) suggesting that the female functionality was not altered. Pollen maturation and morphology were severely influenced in transgenic plants; therefore, the abnormality in male fertility was established as a major cause for low seed-set rate. A histological analysis in the stamen development was performed to further understand the role of male sterility in seed-set. According to Zhang and Wilson (2009), the rice anther development is divided into 14 stages. The developmental defects were not detected in anthers unless the genes were downregulated until stage 8b. At this stage, the tetrads with four haploid microspores were formed, the middle cell layer degenerated, and the endothecium became narrower in all plants (Figure 6A-E). At stage 9, the young microspores were released from the tetrads. The microspores in the wild-type and Ubi:OsMAGO1-RNAi transgenic plants (M1L1) had large nuclei, and homogeneous cytoplasmic constituents were densely stained (Figure 6F-G). On the other hand, the RNAi knockdowns of OsMAGO1OsMAGO2 double (M2L6), OsY14a single (YaL4) or OsMAGO1OsMAGO2OsY14a triple gene (MYaL2), showed more vacuolated microspores that stained less as compared to the wild-type (Figure 6H-J). Specifically, typical falcate pollen grains were formed. At stage 10, the wild-type and M1L1 tapetum appeared to undergo degradation. The microspores were larger and more vacuolated as compared to the WT (Figure 6K and L). In the M2L6, YaL4 or MYaL2 knockdowns, the vacuolated microspores were irregular and shrunken, the tapetum became swollen and broken irregularly (Figure 6M-O). Thus, the anther

lobes were filled with the debris of abolished microspores and cytosolic constituents of the tapetum. At stage 13, the wild-type and M1L1 tapetal layer and the endothecium were completely degraded, and round and densely stained mature pollen grains were formed (Figure 6P and Q). This showed that the normal microspores contain starch, lipids, and other storage metabolites, and they are important for pollen viability and function. However, anther wall layers persisted at this stage in M2L6, YaL4 or MYaL2 knockdowns. The entire endothecium and the partial tapetum were maintained, and most of the pollen grains disintegrated into debris (Figure 6R-T), thus, leading to defect in pollen maturation and morphology. Therefore, OsMAGO1 and OsMAGO2, OsY14a and their heterodimers OsMAGO1 (or 2)-OsY14a play an important role in anther development.

Rice MAGO and Y14 Genes Affect Transcript Levels of Putative Target Genes

To determine the molecular basis of phenotypic variation in the knockdowns of rice MAGO and Y14 genes, we investigated the effects of EJC disruption on the transcript levels of randomly selected genes that were involved in vegetative, flower development and embryogenesis. For this purpose, we designed gene-specific primers flanking full coding region or covering all exons for each gene (Table S4). In RT-PCR, the alteration of mRNA abundance of the investigated genes without any defects in splicing was predominant in Ubi:OsMAGO2-CDS-RNAi (M2L6), Ubi:OsY14a-RNAi (YaL4) and Ubi:OsMAGO1-CDS-OsY14a-RNAi (MYaL2) with downregulation of OsMAGO1OsMAGO2 and OsY14a genes in comparison to wild-type and transgenic controls (M1L1 with a severe downregulation of OsMAGO1 and YaL7 without any downregulation of OsY14a) (Figure S7). The genes showing the downregulation of mRNA expression were: OsGA20ox2 (gibberellic acid (GA) 20-oxidase 2; Qiao and Zhao, 2011), OsGAMYB (a R2R3MYB transcription factor as a positive GA-signaling component; Kaneko et al., 2004); OsEUI (elongated uppermost internode; Zhu et al., 2006), OsCIPK23 (calcineurin B-like interacting protein kinase 23; Yang et al., 2008), OsC6 (encoding a lipid transfer protein; Zhang et al., 2010a), OsTDR (tapetum degeneration retardation; Li et al., 2006), OsCSA (carbon starved anther; Zhang et al., 2010b) and *OsMST8 (monosaccharide transporter* 8; Mamun et al., 2006). However, the *OsPTC1* transcripts (*persistent tapetal cell 1*; Li et al., 2011) increased. Furthermore, the mature mRNA expressions of some genes were not altered in these knockdowns. These were: *OsRBP (dsRNA binding protein*; Tang et al., 2002), *OsRab5a* (Wang et al., 2010), *OsGSR1 (GA-stimulated gene*; Wang et al., 2009), *OsSIN (short internodes*; Han et al., 2005), *OsMSP1 (multiple sporocyte 1*; Li et al., 2011), *OsINV4* (rice anther-specific cell wall invertase gene; Oliver et al., 2005), *OsLEAFY* (NM_001060277), *OsMADS18* (Fornara et al., 2004), *OsMADS8* (Kang et al., 1997) and *OsACTIN1* (NM_001057621). Interestingly, multiple splicing products of the *OsUDT1 (undeveloped tapetum 1*; Jung et al., 2005) gene were visible in the downregulation mutants of *OsMAGO1OsMAGO2* and *OsY14a* genes (Figure S7).

The expression of these genes was also investigated (highlighted in the red box, Figure S7) in *Ubi:OsY14b-RNAi* callus (YbL1), which showed increased expression of *OsRBP* in comparison to the WT. On the other hand, the mature transcripts of *OsEUI*, *OsCIPK23*, *OsGAMYB* and *OsCSA* genes were severely downregulated, and *OsRab5a*, *OsGSR1*, *OsSIN*, *OsMSP1*, *OsMST8* and *OsACTIN1* expressions seemed to be remained unchanged. The expression of other genes was not detectable in the callus.

Rice MAGO and Y14 Regulate the Splicing of the OsUDT1 Transcripts

The occurrence of multiple splicing products of the *OsUDT1* transcripts in the knockdowns of the rice EJC genes (Figure S7) indicated that the splicing of this gene was affected in these RNAi lines. In order to ascertain the nature of these transcript species, we cloned and sequenced the RT-PCR products from both the wild-type rice and *Ubi:Y14a*-RNAi plants. As compared with the expected mature transcripts, three abnormal transcript species (type I, II and III) of the *OsUDT1* gene were produced (Figure 7A). Intron retention was observed in the Type I species, exon skipping events occurred in the Type II and III transcript species. Interestingly, the first exon was mis-spliced resulting in different size of "the first intron" observed in the Type II and III transcript species. These results suggested that these EJC subunits play a critical

role in faithful splicing of the OsUDT1 pre-mRNA.

To further evaluate this, we examined the expression level of the pre-mRNA and mRNA of the OsUDT1 gene by qRT-PCR using primers to amplify both intron-exon and exon-exon junctions (Figure 7B and C). A reduction in the amount of the mature OsUDT1 transcripts in transgenic plants M2L6, YaL4 and MYaL2 was apparent as compared to the wild-type (Figure 7B). The variability of pre-mRNA levels over the length of the OsUDT1 gene (Figure 7C) further suggested an abnormal splicing of the OsUDT1 transcripts in knockdowns of rice EJC genes. We next synthesized the fusion proteins of rice MAGO and Y14 with GST (Glutathione S-transferase), respectively, and incubated them with pre-mRNA of 14 genes (see Methods). All of these fusion proteins could specifically bind to the OsUDT1 pre-mRNA after elution as demonstrated by saturated RT-PCR amplification (Figure S8). Surprisingly, we found that the rice MAGO or Y14 proteins could bind to all regions of the OsUDT1 pre-mRNA when a high dosage of each pre-mRNA segment was incubated with each GST-fusion protein (Figure 8A). To clarify this, we did competitive binding assays through reducing the concentrations of the EJC subunits. Once a low concentration of GST-OsMAGO1 (Figure 8B) or GST-OsY14a (Figure 8C) was input, these proteins competitively bound to 'the first exon region' of the OsUDT1 transcripts. Similar was observed for GST-OsMAGO2 and OsY14b (Figure S9A and B). The capability of binding to pre-mRNA, particularly the preferential binding to 'the first exon region', might form a key basis for regulating the splicing of the OsUDT1 transcripts by these EJC subunits.

DISCUSSION

MAGO and Y14 are the core components of EJC and play essential roles in the post-transcriptional processes and organism development in animals. However, these processes are poorly understood in plants. In the present study, we show the divergence of rice *MAGO*- and *Y14*-duplicated gene pairs, and establish that they are all essential to growth and development of multiple organs. Furthermore, divergent expressions in response to stresses imply a clear divergence of these genes for

adaptation. Moreover, the *OsUDT1*, a key regulatory gene in stamen development was found to be a post-transcriptional splicing target of the EJC subunits in rice.

Functional Divergence of MAGO- and Y14-Duplicated Gene Pairs in Rice

We found that OsMAGO1 and OsMAGO2 were highly conserved (> 93%) and their genes had a similar and constitutive expression pattern during rice development. Moreover, single-gene-knockdowns of either OsMAGO1 or OsMAGO2 did not show any phenotypic variation while obvious phenotypic deviations from the wild type were observed in the double OsMAGO1OsMAGO2 knockdowns. Therefore, both OsMAGO1 and OsMAGO2 are redundant in rice development (Figure 9). The OsMAGO1OsMAGO2 knockdowns affected floral growth and showed retarded vegetative growth. The lemma and palea in these knockdowns became larger while the stamen and its filament became shorter. Furthermore, the organ size appeared to correlate to cell size in these organs, indicating that rice MAGO could affect cell expansion. These knockdowns further showed inhibited stamen development, altered pollen morphology and inhibited pollen maturation process. The cytohistological assays we conducted revealed that normal degradation and absorption of both endothecium and tapetum were inhibited, thus, leading to defect in pollen maturation and morphology. Defect in pollen development was also observed in *hapless1* (atmago) and AtMAGO-RNAi plants in Arabidopsis (Johnson et al., 2004; Park et al., 2009), and in the knockdowns of Mv-MAGO in Marsilea vestita (Boothby and Wolniak, 2011; van der Weele et al., 2007). However, the transgenic rice plants in our study did not show any defects in the floral meristem and seed development as were observed in Arabidopsis (Park et al., 2009). Thus, MAGO genes probably went through functional conservation and diversification in plants.

Unlike the paralogous *OsMAGO1/2* gene pair, the *OsY14a/b* pair showed distinct divergence that was supported by dramatic sequence variations (< 47%) and distinct differential gene expression patterns during rice development. *OsY14a* had a broad expression domain similar to that of the *OsMAGO1/2* pair; therefore, severe downregulation of this gene led to similar phenotypic variation as observed in

OsMAGO1OsMAGO2 double knockdowns. Contrastingly, *OsY14b*, was only expressed in embryonic callus and earlier vegetative and floral development. Moreover, OsY14b protein was under positive selection, and the two paralogs became extensively diverged in their sequences (Gong et al., 2014). These facts together support a specialization of function for this gene. Similar to the mutation in *AtY14* in *Arabidopsis* (Park et al., 2009), we also observed a lethal phenotype associated with failure in shoot induction from the embryonic callus in downregulating *OsY14b*. Thus, we concluded that *OsY14b* plays a key role in embryo development and early embryonic organogenesis (Figure 9). This function could not be replaced by *OsY14a*, suggesting that the two paralogous genes underwent dramatic functional divergence after duplication.

Similar mutational phenotypic variations were observed in the knockdowns of *OsMAGO10sMAGO2* or *OsY14a*, suggesting that they might exert their roles via forming heterodimers. The role of MAGO-Y14 heterodimer has not been demonstrated possibly due to its lethality in a species having a single copy. Due to the essential role of *OsY14b*, it is hard to reveal the developmental role of OsY14b and its heterodimers with OsMAGO1 and OsMAGO2 in rice. Nonetheless, using RNAi technology, we generated the triple gene (*OsMAGO10sMAGO20sY14a*) downregulated mutants. These transgenic rice plants showed enhanced phenotypic variations that occurred in *Ubi:OsMAGO10sMAGO2*-RNAi and *Ubi:OsY14a*-RNAi plants. As demonstrated in animals (Mohr et al., 2001; Kawano et al., 2004; Parma et al., 2007; Lewandowski et al., 2010), rice MAGO and Y14 form a complex to exert their role in the same or related developmental pathways that control growth, development and reproduction.

Rice MAGO and Y14 Selectively Regulate the Splicing of the *OsUDT1* **Transcript**

Abnormal growth and development in the transgenic rice plants can be attributed to the abnormal expression of related genes. This was consistent with the previous observation (Qiao and Zhao, 2011) that downregulation of *OsGA20ox2* reduced the plant height in rice. The multiple defects in pollen development and male sterility are

thought to be associated with abnormal expression of various genes, such as *OsCSA* encoding an MYB domain protein that regulates sugar partitioning (Zhang et al., 2010b), *OsGAMYB* (Kaneko et al., 2004), *OsUDT1* (Jung et al., 2005), *OsTDR* (Li et al., 2006) and *OsC6* (Zhang et al., 2010a). Another rice gene, *OsINV4*, is involved in sucrose accumulation and pollen sterility in rice (Oliver et al., 2005) while the gene *OsMSP1* controls early sporogenic development (Li et al., 2011). However, the expression of neither of these genes was affected by downregulating the rice EJC genes. Our observations also support that multiple regulatory pathways are involved in pollen development in rice (Wang et al., 2013). The interconnections of exon junction complex subunits are important for the correct gene expression in *Arabidopsis* (Mufarrege et al., 2011). This is corroborated by our data, which shows that rice EJC subunits may fulfill their essential roles by regulating a substantial set of gene expression.

The altered expression levels of these genes are unknown; however, the altered splicing of the OsUDT1 transcripts was clearly supported by the occurrence of multiple splicing products of this gene in our rice EJC knockdowns. Additional sequencing suggested that the regulation on the OsUDT1 transcript splicing by rice MAGO proteins and OsY14a was fulfilled in a combined manner consisting of intron retention, exon skipping and recognition of alternative splice sites in the first exon. Furthermore, we found that OsMAGO1/2, OsY14a and their heterodimers could bind to the OsUDT1 pre-mRNA, particularly at the first exon. In line with our observations, the EJC subunits also control the transcript splicing of the *mitogen-activated protein* kinase (MAPK) gene in Drosophila (Ashton-Beaucage et al., 2010; Roignant and Treisman, 2010). In eukaryotic cells, a nonsense-mediated mRNA decay (NMD), as a surveillance mechanism, eliminates mRNAs that contain nonsense mutations or acquire premature termination codons because of aberrant splicing (Chang et al., 2007). Therefore, NMD is an effective safeguard for eliminating aberrant gene expression (Chang et al., 2007; Chuang et al., 2013; Kalyna et al., 2012; Nyikó et al., 2013). However, the aberrant OsUDT1 transcripts were specifically maintained despite the deletions of the rice MAGO and Y14 genes. Contrastingly, the expression

levels of most altered genes was affected either by down- or up-regulation, suggesting a role for these EJC subunits in transcriptional regulation. Considering the nature of these EJC subunits, the ancillary subunits might be essential for the transcriptional regulatory role. This was shown by the interaction of PFMAGO with MPF2, a MADS-domain regulatory factor in *P. floridana* (He et al., 2007). Alternatively, the observed transcriptional regulation might be a consequence of the abnormal splicing of the *OsUDT1*, an upstream regulator in network of male fertility in rice (Wang et al., 2013). Nevertheless, further investigations in rice are required to support these notions.

The expression of genes from various developmental pathways was affected by downregulating rice MAGO and Y14 genes, suggesting no specificity of the EJC targets in rice. However, not all monitored gene expression was altered on disruption of either MAGO or Y14 genes in rice, suggesting that the gene expression in general does not require the EJC, hence arguing the specificity and priority of the EJC targets in rice. However, in animals the EJC is proposed to bind to intron-containing genes (Le Hir et al., 2000), and the intron length determines the EJC's effect on splicing in Drosophila ssp. (Ashton-Beaucage et al., 2010; Roignant and Treisman, 2010). The presence of the alternative splicing sites within the large introns containing repetitive sequences could interfere with the splicing of the introns they occupy (Ponicsan et al., 2010). However, bias for long introns in human target units was not detected (Michelle et al., 2012), nor was found in rice (Table S4). The target specificity of the rice EJC subunits is not clear yet, but the *OsUDT1*, the upstream key regulator for male fertility (Jung et al., 2005), is apparently the direct target for the rice EJC subunits. The discrepancy and diversity of mechanisms for EJC target selection between different species suggest that they act in a species-specific evolutionary mode.

Therefore, our study suggests that *MAGO* and *Y14* genes were separately duplicated in cereals, and their sequence divergence shaped their functional evolution. *OsMAGO1* and *OsY14a* partitioned their fundamental roles in growth, development

and reproduction through specific regulations of gene expression in rice, while *OsY14b* specialized in embryo organogenesis (Figure 9). Moreover, both *OsMAGO2* and *OsY14b* evolved to be sensitive to external changes. These findings in rice implicate the importance of these EJC genes in cereal development and adaptive evolution.

MATERIALS AND METHODS

Plant Materials

The rice *O. sativa* L. cv. 'Zhonghua 10' and its transgenic plants generated in the present work were cultivated in a growth chamber under short-day conditions (10/14 hrs light/dark cycle with 28/25°C accordingly) with a relative humidity of 50 per cent. *Nicotiana benthamiana* plants were grown in an incubator (RXZ-380C, Ningbo, China) under long-day conditions (16/8 hrs light/dark cycle) with a constant temperature of 22°C.

Abiotic Stresses and Hormonal Treatments

For abiotic stresses, 12-day-old rice seedlings on 1/2 MS were irrigated with 20% Mannitol or 200 mM NaCl solution. Hot or cold stresses were provided by placing the seedlings in an incubator maintained at 4 or 42°C, respectively. Seedlings were sampled at 0, 1, 4, 8, 12, 24, 36 and 48 hrs after treatments. For hormonal treatments, seedlings were treated with 100 μ M ABA (abscisic acid), 1 μ M BR (brassinolide), 10 μ M GA₃ (gibberellic acid 3), and 10 μ M IAA (indole-3-acetic acid), respectively, and then sampled at 0, 1, 3, 8 and 24 hrs. ABA (A1049), BR (E1641), GA₃ (G7645), and IAA (I2886) were purchased from Sigma-Aldrich (Sigma, St. Louis, USA).

RT-PCR Analyses

Total RNA from the tissues indicated was isolated using the Trizol Kit (Invitrogen, USA), and then treated with RNase-Free DNase (Promega, USA) to remove genomic DNA contamination. First-strand cDNA was synthesized using the MLV RT-PCR Kit (Invitrogen, USA) in a 20.0 μ l reaction with the oligo (dT)₁₇ primer. qRT-PCR was

performed using the SYBR *Premix Ex Taq*TM (Tli RNaseH plus) Kit (Takara, Dalian, China) in an Mx3000PTM Real-Time PCR instrument (Stratagene, Germany) in a final 25.0 μ L volume. The reactions were performed at 95°C for 30 s, 40 cycles of 95°C for 5 s, and 60°C for 40 s, and then 60 s at 95°C, 30 s at 60°C and 30 s at 95°C , and one cycle for melting curve analysis. Experiments were performed using three independent biological samples. The mean and standard deviation are presented. Semi-quantitative RT-PCR was performed using the *ExTaq* system (Takara, Dalian, China) in a final 25.0 μ l volume. The reactions were performed at 95°C for 3 min, 24, or 28 or 30 cycles of 95°C for 30 s, 55°C for 30 s, 72°C for 2 min, and 72°C for 10 min. The PCR products were separated on a 1.2% agarose gel. A typical gel from three experiments of independent biological samples is presented. *OsACTIN1* gene was used as an internal control.

Plasmid Construction

The cDNAs containing open reading frames (ORFs) were cloned into the pGEM-T EASY vector (Promega, USA) and sequenced (Gong et al., 2014). To generate constructs for RNAi, each coding region of *OsMAGO1* and *OsMAGO2*, *3'UTR* of *OsMAGO1*, and the gene-specific fragment of *OsY14a* or *OsY14b* was respectively inserted into the vector *pTCK303* driven by the ubiquitin promoter (Wang et al., 2004) to make the *pTCK303-OsMAGO1CDS*, *pTCK303-OsMAGO2CDS*, *pTCK303-OsMAGO1-3'UTR*, *pTCK303-OsY14a* and *pTCK303-OsY14b* plasmids. The *pTCK303-OsMAGO1CDS-OsY14a* was also made for triple gene knockdowns. For subcellular localization, the ORF of rice *MAGO* and *Y14* was cloned into the expression vector *pCAMBIA1302* to generate *pCAMBIA1302-OsMAGO1*, *pCAMBIA1302-OsY14a* and *pCAMBIA1302-OsY14b* using primers with restriction digestion sites *Nco* I and *Spe* I. The ORF of *OsMAGO2* was cloned into expression vector *pSuper1300* to generate *pSuper1300-OsMAGO2* using gene-specific primers containing *Xba* I and *BamH* I cutting sites. For the bimolecular fluorescence complementation (BiFC) experiments, the ORFs from rice *MAGO* and *Y14* were cloned into the *pSPY35SNE* and *pSPY35SCE* vector (Walter et al., 2004) to generate *pSPYNE/CE-OsMAGO1*, *pSPYNE/CE-OsMAGO2*, *pSPYNE/CE-OsY14a* and *pSPYNE/CE-OsY14b*, respectively. Glutathione S-Transferase (GST) fusion proteins were produced by inserting the ORF of rice *MAGO* and *Y14* into the pGEX-4T vector to generate *pGEX-4T-OsMAGO1*, *pGEX-4T-OsMAGO2*, *pGEX-4T-OsY14a* and *pGEX-4T-OsY14b*, respectively.

Sequencing Analyses and Primer Synthesis

All constructs (made) and products of the RT-PCR assays were commercially sequenced. The primers used in the present work (shown in Table S5) were commercially synthesized by the Beijing Genomic Institute and by Taihe Biotechnology (Beijing, China).

Rice Transgenic Analyses

Rice embryonic calli were induced from germinated seeds on N_6D_2 solid medium and inoculated with *Agrobacterium tumefaciens* EHA105 as previously description (Xu et al., 2005). Plantlet regeneration rate was summarized in Table S1.

Yeast Two-Hybrid Assay

The indicated combination of the bait and prey plasmids was co-transformed into the yeast strain AH109. The non-lethal β -galactosidase activity was performed on the SD/-Trp-Leu-His-Ade plates. The o-nitrophenyl- β -D-galactoside (ONPG) was used as a substrate to quantify the interacting affinity. The procedures described in Yeast Protocols Handbook (Clontech, Mountain View, USA) were followed.

Transient Protein Expression Analyses

For subcellular localization, the derived *pCAMBIA1302* constructs were first transformed into the *A. tumefaciens* EHA105 cells, and then introduced into the epidermal cells of *N. benthamiana* by agroinfiltration. The empty *GFP* vector (*pCAMBIA1302*) was infiltrated as a control. For BiFC assay, the resulting

pSPY35SNE and *pSPY35SCE* plasmids were transformed into *A. tumefaciens EHA105*, respectively, and then the NE- and CE-fused proteins were co-expressed in the epidermal cells of *N. benthamiana* by agroinfiltration (Walter et al., 2004). The GFP or YFP signal was observed under a confocal laser scanning microscope (Olympus FV1000 MPE, Japan). The YFP signal intensity was quantified using ImageJ (http://rsb.info.nih.gov/nih-image; Abramoff et al., 2004).

Anther Histochemical and Microscopic Analysis

For anther cytohistological assay, the spikelets of various anther developmental stages were fixed with FAA (70% ethanol: 5% glacial acetic acids: 3.7% formaldehyde) for 24 h at room temperature. Fixed anthers were dehydrated through an ethanol series, and then embedded into Spurr's resin (Sigma-Aldrich, St. Louis, USA) and polymerized at 60°C for 24 hrs. The sample blocks were sectioned into 1 µm thick slices with a microtome (Leica ultracut R, Germany) and stained with 0.1% toluidine blue O (Merck, Darmstadt, Germany). Pollen from mature anthers was dissected into a drop of iodine/potassium iodide solution. The images were captured with a Zeiss Imager A1 Digital Camera System (Zeiss, Germany). For scanning electron microscopic (SEM) analyses, lemma, anthers and filaments from mature florets were fixed using FAA. Then they were dehydrated through an ethanol series followed by replacing them with an isoamyl acetate series and drying with liquid carbon dioxide. Images were captured with a scanning electron microscope (Hitachi S-800, Japan) at 10 KV. Florets and organs were photographed using a Nikon SMI 1000 microscopic digital camera. Organ and cell size was measured by using the software Carl Zeiss Vision Axiovision Rel. 4.7 (http://microscopy.zeiss.com).

GST-Fusion Protein Induction and Abstraction

The GST fusion protein plasmids and the empty pGEX-4T-1 vector were transformed into *E. coli* Rosetta (DE3) (TransGen, China), and protein expression was induced by a certain concentration of IPTG. The soluble GST fusion proteins were extracted and immobilized onto glutathione sepharose beads (Amersham Biosciences, USA).

Pre-mRNA Binding with GST-Fusion Proteins

Genomic sequence of each gene was amplified using PCR amplification, and was constructed into T-plasmid (*pEASY-T*1 or *pEASY Blunt Zero* vector, TransGen). Sense pre-mRNA was transcribed from the plasmid after linearization by T7 promoter (*In Vitro* Transcription T7 Kit, Takara, Dalian, China). The pre-mRNA binding with GST-fusion proteins was performed as previously described (Ramasamy et al., 2006). To search the pre-mRNA target of rice MAGO and Y14, 250 ng each pre-mRNA was incubated with 1 ug of each GST-fusion protein. For a competitive binding assay, 125 ng of each intron and exon pre-mRNA were mixed and incubated with different concentrations (2 μ g, 1 μ g and 0.5 μ g) of each GST-fusion protein as indicated. Reverse transcription of purified pre-mRNA was performed by random primer (Hexadeoxyribonucleotide mixture, pd(N)₆; Takara, Dalian, China) and used for RT-PCR to detect each interacted pre-mRNA with GST fusion protein.

Supplemental Data

The following materials are available in the online version of this article.

Figure S1. Gene Expressions of Rice *MAGO* and *Y14* under Different Types of Stresses.

Figure S2. Interaction of Rice MAGO and Y14 Proteins in Yeast.

Figure S3. Genotyping Analyses of the RNAi Transgenic Rice Plants.

Figure S4. Variation in Cell Size in the Wild Type and Transgenic Rice Plants.

Figure S5. *Ubi:OsY14b*-RNAi Transgenic Rice Plants.

Figure S6. Phenotype of OsMAGO1-3'UTR-RNAi Transgenic Rice Plants.

Figure S7. Gene Expression Profiles in the Transgenic Rice Plants.

Figure S8. Rice MAGO and Y14 Specifically Bind to the OsUDT1 Pre-mRNA.

Figure S9. OsMAGO2 and OsY14b Proteins Bind to the OsUDT1 Pre-mRNA.

 Table S1. Transformation of Rice RNAi Lines.

Table S2. Phenotypic Variations in RNAi Transgenic Rice Plants.

Table S3. Ovary Fertility Alteration in Transgenic Rice Plants.Table S4. Gene Information Used in Expression Studies.Table S5. List of Primers Used in the Present Study.

ACKNOWLEDGEMENTS

We thank Dr. Kang Chong for his generous providing the vector plasmid to prepare constructs in transgenic rice. The assistances of Mr. Yinghou Xiao in SEM analysis, Dr. Li Wang in rice transgenic analyses and Mrs. Fengqin Dong in transverse sections are also acknowledged.

Figure Legends

Figure 1. Expression Patterns of Rice *MAGO* and *Y14* Genes during Rice Development.

Callus: 2-week-old on 1/2 MS medium; Shoots (S1-S7): 1- to 7-day-old seedlings (without roots) on 1/2 MS medium; Roots: 12-day-old seedlings on 1/2 MS medium; Leaf: flag leaves of mature plants at heading stage; G-L-L (mixture of glumes, lemmas and lodicules); Stamen and Pistil from mature florets; Em1-Em12: embryo at 1, 3, 6 and 12 days after fertilization. *OsACTIN1* was used as an internal control. The expressions were detected with three independent biological samples. The expression for each gene in S7 was set to 1. The average expression and the standard deviation are presented.

Figure 2. Transient Expression of the Rice MAGO and Y14 Proteins.

(A-E) Subcellular localization. Expression of the fusion protein (A) OsMAGO1-GFP, (B) OsMAGO2-GFP, (C) OsY14a-GFP and (D) OsY14b-GFP. (E) Expression of GFP protein as a control. Bars = 50 μ m. (F-J) Rice MAGO-Y14 heterodimerization revealed in bimolecular fluorescence complementation assays. Co-expression of (F) OsMAGO1-YFPc and OsY14a-YFPn, (G) OsMAGO2-YFPc and OsY14a-YFPn, (H) OsMAGO1-YFPc and OsY14b-YFPn, and (I) OsMAGO2-YFPc and OsY14b-YFPn. The detection of YFP signals indicates an interaction of the combined proteins. (J) Co-expression of YFPc and OsY14a-YFPn proteins as a negative control. Bars = 50 μ m. Quantification of fluorescence intensity of YFP signals in nucleus (Nu) and cytoplasm (Cp) is presented for each merged image. N, numbers of cells quantified.

Figure 3. Phenotypic Comparisons of the Wild-Type and *OsY14a*-RNAi Transgenic Rice Plants.

(A) Rice plants at heading stage of wild-type (WT, left) and *OsY14a*-RNAi line 4 (YaL4, right). Bars = 20 cm. (B) Internodes (I-V) and panicle of WT and YaL4 after seeds maturation. Bars = 20 cm. (C) Size quantification of the internode (I to V, where I is the uppermost) and panicle (Pa) between WT and YaL4. The significance was evaluated by two-tailed *t*-test. * indicates P < 0.05, and ** indicate P < 0.01. (D and E) Floret of WT and YaL4. Bars = 1 mm. (F and G) Epidermal cells on lemma of WT and YaL4. Bars = 10 mm. (F and G) Epidermal cells on lemma of WT and YaL4. Bars = 10 mm. (J and K) Pistil of WT and YaL4. Bars = 1 mm. (L and M) Stamen of WT and YaL4. Bars = 1 mm. Glumes (Gl), lemma (Le), palea (Pa), stamen (Sta), anther (An), filament (Fi), pistil (Pi), stigma (Sti) and ovary (Ov) are indicated in D, E and H-M. (N and O) Cells on filament of WT and YaL4 with SEM. Bars = 50 μ m. (P and Q) Cells on anther of WT and YaL4 with SEM. Bars = 50 μ m. (P and W) Cells on anther of WT and YaL4 with SEM. Bars = 20 μ m in (T and U), 20 μ m in (V and W). (X and Y) Germ pore of WT and YaL4 with SEM. Bars = 20 μ m.

Figure 4. Phenotypic Variations in *OsMAGO10sMAGO2* Downregulated Transgenic Rice Plants.

(A) Internodes (I-V) and panicle comparison of the wild type (WT, left), M1L7 (*Ubi:OsMAGO*1-CDS-RNAi, middle) and M2L6 (*Ubi:OsMAGO*2-CDS-RNAi, right) after seed maturation. Bars = 20 cm. (B) Size quantification of the internode (I to V, where I is the uppermost) and panicle (Pa) between WT, M1L7 and M2L6. The significance was evaluated by two-tailed *t*-test. ** indicate P < 0.01. (C-E) Floret of WT, M1L7 and M2L6. Bars = 1 mm. (F-H) Cells on lemma of WT, M1L7 and M2L6

with SEM. Bars = 50 μ m. (I-K) Pistil of WT, M1L7 and M2L6. Bars = 1 mm. (L-N) Stamen of WT, M1L7 and M2L6. Bars = 1 mm. Anther (An), filament (Fi), stigma (Sti) and ovary (Ov) are indicated in I-N. (O-Q) Cells on filament of WT, M1L7 and M2L6 with SEM. Bars = 50 μ m. (R-T) Cells on anther of WT, M1L7 and M2L6 with SEM. Bars = 50 μ m. (U-W) The I₂-KI staining pollen grains of the WT, M1L7 and M2L6. (X-Z) Pollen of WT, M1L7 and M2L6 with SEM. Bars = 20 μ m.

Figure 5. Phenotypic Variations of *OsMAGO1OsMAGO2OsY14*a Downregulated Transgenic Rice Plants.

(A) Gene expression in *Ubi:OsMAGO1-CDS-OsY14a*-RNAi transgenic lines. Hygromycin gene expression (HYG) detected by RT-PCR. OsACTIN1 was used as an internal control. Three independent biological samples were used for detecting expression. The expression for each gene in wild-type (WT) was set to 1. The average expression and the standard deviation are presented. (B) Rice plant at heading stage of WT (left) and MYaL2 (*OsMAGO1OsMAGO2OsY14a* knockdown, right). Bars = 20 cm. (C) Internodes (I-V) and panicle of WT (left) and MYaL2 (right) after seed maturation. Bars = 20 cm. (D) Size quantification of the internode (I to V, where I is the uppermost) and panicle (Pa) between WT and MYaL2. The significance was evaluated by two-tailed t-test. * indicates P < 0.05, and ** indicate P < 0.01. (E and F) Floret of WT and MYaL2. Bars = 1 mm. (G and H) Cells on lemma of WT and MYaL2 with SEM. Bars = 50 μ m. (I and J) Artificial opened floret of WT and MYaL2. Bars = 1 mm. (K and L) Pistil of WT and MYaL2. Bars = 1 mm. (M and N) Stamen of WT and MYaL2. Bars = 1 mm. Glumes (Gl), lemma (Le), palea (Pa), stamen (Sta), anther (An), filament (Fi), pistil (Pi), stigma (Sti) and ovary (Ov) are indicated in E-N. (O and P) Cells on filament of WT and MYaL2 with SEM. Bars = $50 \mu m$. (Q and R) Cells on anther of WT and MYaL2 with SEM. Bars = $50 \mu m$. (S and T) The I₂-KI staining pollen grains of the WT and MYaL2. (U and V) Pollen of WT and MYaL2 with SEM. Bars = $20 \,\mu m$.

Figure 6. Transverse Sections of Anthers in Wild-Type and Downregulated Mutants.

27

Four stages of anther development in wild-type (WT) and transgenic plants were compared. Images in (A, F, K and P) are WT; (B, G, L and Q) are the *OsMAGO1* downregulated plant M1L1; (C, H, M and R) are the *OsMAGO1/2* downregulated plant M2L6; (D, I, N and S) are the *OsY14a* downregulated plant YaL4; (E, J, Q and T) are the *OsMAGO1OsMAGO2OsY14a* downregulated plants MYaL2. (A-E), stage 8b; (F-J), stage 9; (K-O), stage 10; (P-T), stage 13. Ep, epidermis; En, endothecium; Tds, tetrads; Ta, tapetum; Msp, microspore; Mp, mature pollen. Bars = 50 µm.

Figure 7. Rice MAGO and Y14 Affect the OsUDT1 Transcripts.

(A) The *OsUDT1* transcript species from the knockdowns of the EJC genes. The pre-mRNA and mature mRNA are given as controls. Grey rectangles, UTRs; white rectangles, exons/E; straight lines, introns/I. The numbers represent the length of the 5'UTR and E1. Three abnormal transcript species were obtained: I type; the first intron was retained because of the GC-AG boundary, II type, lacking partial E1 and entire E3, and III type, lacking partial E1, the whole E2 and E3. (B) The *OsUDT1* mature mRNA level is reduced in knockdowns of rice EJC genes. Primers spanning each exon-exon junction were used in qRT-PCR. (C) Pre-mRNA variations of the *OsUDT1* gene in knockdowns of rice EJC genes. The total RNAs from the inflorescence of the wild-type (WT) and three RNAi lines M2L6, YaL4 and MYaL2 as indicated were used for qRT-PCR using primers spanning each exon-intron junctions. In B and C, the MADS-box gene *OsMAGO18* was used as a control. Three independent biological samples were used, and error bars represent standard deviations. The significance was evaluated by two-tailed *t*-test. * indicates P < 0.05, and ** indicate P < 0.01.

Figure 8. Rice MAGO and Y14 Bind to the OsUDT1 Pre-mRNA.

(A) Pre-selection of binding region. Saturated RT-PCR was performed using each exon (E) and intron (I) pre-mRNA from the GST-fusion protein beads indicated. The "No template" and "pre-mRNA" were used as negative controls, while the plasmids and cDNAs were used as positive controls. 1 µg GST, Glutathione beads (GST-Beads),

GST-MAGO and GST-Y14, were incubated with 250 ng of the pre-mRNAs as indicated. (B and C) Pre-mRNA competitive binding assays. The mixture of each exon (E) and intron (I) pre-mRNA fragment (125ng each) was incubated with the indicated concentrations of GST-OsMAGO1 (B) or GST-Y14a (C). Relative enriched level of the bound pre-mRNA was shown by qRT-PCR assays. The bound E1 pre-mRNA level was set to 1. Each experiment was performed with three independent samples, and error bars represent standard deviations.

Figure 9. Functional divergence of OsMAGO1/2 and OsY14a/b in rice.

M1/2 and Ya/b are abbreviated from of OsMAGO1/2 and OsY14a/b. Solid patterns: wild-type M1/2 or Ya/b; dotted patterns: mutants m1/2 and ya/b (null or knockdown). Blue lines represent heterodimerization. Only the preferential heterodimerizations are shown.

LITERATURE CITED

Abramoff MD, Magelhaes PJ, Ram SJ (2004) Image processing with ImageJ. Biophotonics Int **11**: 36-42.

Alachkar A, Jiang D, Harrison M, Zhou Y, Chen G, Mao Y (2013) An EJC factor RBM8a regulates anxiety behaviors. Curr Mol Med **13**: 887-899.

Ashton-Beaucage D, Udell CM, Lavoie H, Baril C, Lefrançois M, Chagnon P, Gendron P, Caron-Lizotte O, Bonneil E, Thibault P, Therrien M (2010) The exon junction complex controls the splicing of *mapk* and other long intron-containing transcripts in *Drosophila*. Cell **143**: 251-262.

Boothby TC, Wolniak SM (2011) Masked mRNA is stored with aggregated nuclear speckles and its asymmetric redistribution requires a homolog of mago nashi. BMC Cell Biol **12**: 45.

Boswell RE, Prout ME, Steichen JC (1991) Mutations in a newly identified *Drosophila melanogaster* gene, *mago nashi*, disrupt germ cell formation and result in the formation of mirror-image symmetrical double abdomen embryos. Development **113**: 373-384. **Chang YF, Imam JS, Wilkinson MF** (2007) The nonsense-mediated decay RNA surveillance pathway. Annu Rev Biochem **76**: 51-74.

Chen YR, Shaw JF, Chung MC, Chu FH (2007) Molecular identification and characterization of *Tcmago* and *TcY14* in *Taiwania (Taiwania cryptomerioides)*. Tree Physiol **27**: 1261-1271.

Chuang TW, Chang WL, Lee KM, Tarn WY (2013) The RNA-binding protein Y14 inhibits mRNA decapping and modulates processing body formation. Mol Biol Cell 24: 1-13.

Fornara F, Parenicová L, Falasca G, Pelucchi N, Masiero S, Ciannamea S, Lopez-Dee Z, Altamura MM, Colombo L, Kater MM (2004). Functional characterization of *OsMADS18*, a member of the *AP1/SQUA* subfamily of MADS box genes. Plant Physiol **135**: 2207-2219.

Gong PC, Zhao M, He CY (2014) Slow co-evolution of the MAGO and Y14 protein families is required for the maintenance of their obligate heterodimerization mode. PLoS One **9**: e84842.

Hachet O, Ephrussi A (2001) *Drosophila* Y14 shuttles to the posterior of the oocyte and is required for *oskar* mRNA transport. Curr Biol **11**: 1666-1674.

Han Y, Jiang JF, Liu HL, Ma QB, Xu WZ, Xu YY, Xu ZH, Chong K (2005) Overexpression of *OsSIN*, encoding a novel small protein, causes short internodes in *Oryza sativa*. Plant Sci **169**: 487-495.

He CY, Sommer H, Grosardt B, Huijser P, Saedler H (2007) PFMAGO, a MAGO NASHI-like factor, interacts with the MADS-box protein MPF2 from *Physalis floridana*. Mol Biol Evol **24**: 1229-1241.

Inaki M, Kato D, Utsugi T, Onoda F, Hanaoka F, Murakami Y (2011) Genetic analyses using a mouse cell cycle mutant identifies *magoh* as a novel gene involved in Cdk regulation. Genes Cells **16**: 166-178.

Johnson MA, von Besser K, Zhou Q, Smith E, Aux G, Patton D, Levin JZ, Preuss D (2004) *Arabidopsis hapless* mutations define essential gametophytic functions. Genetics **168**: 971-982.

Jung KH, Han MJ, Lee YS, Kim YW, Hwang I, Kim MJ, Kim YK, Nahm BH, 30 **An G** (2005) Rice *Undeveloped Tapetum1* is a major regulator of early tapetum development. Plant Cell **17**: 2705-2722.

Kalyna M, Simpson CG, Syed NH, Lewandowska D, Marquez Y, Kusenda B, Marshall J, Fuller J, Cardle L, McNicol J, Dinh HQ, Barta A, Brown JWS

(2012). Alternative splicing and nonsense-mediated decay modulate expression of important regulatory genes in *Arabidopsis*. Nucleic Acids Res **40**: 2454-2469.

Kaneko M, Inukai Y, Ueguchi-Tanaka M, Itoh H, Izawa T, Kobayashi Y,

Hattori T, Miyao A, Hirochika H, Ashikari M, Matsuoka M (2004)

Loss-of-function mutations of the rice *GAMYB* gene impair α -amylase expression in aleurone and flower development. Plant Cell **16**: 33-44.

Kang HG, Jang S, Chung JE, Cho YG, An G (1997) Characterization of two rice MADS box genes that control flowering time. Mol Cells **7**: 559-566.

Kataoka N, Diem MD, Kim VN, Yong J, Dreyfuss G (2001) Magoh, a human homolog of *Drosophila* mago nashi protein, is a component of the splicing-dependent exon-exon junction complex. EMBO J **20**: 6424-6433.

Kataoka N, Yong J, Kim VN, Velazquez F, Perkinson RA, Wang F, Dreyfuss G (2000) Pre-mRNA splicing imprints mRNA in the nucleus with a novel RNA-binding protein that persists in the cytoplasm. Mol Cell **6**: 673-682.

Kawano T, Kataoka N, Dreyfuss G, Sakamoto H (2004) Ce-Y14 and MAG-1, components of the exon-exon junction complex, are required for embryogenesis and germline sexual switching in *Caenorhabditis elegans*. Mech Dev **121**: 27-35.

Kim VN, Yong J, Kataoka N, Abel L, Diem MD, Dreyfuss G (2001) The Y14 protein communicates to the cytoplasm the position of exon-exon junctions. EMBO J **20**: 2062-2068.

Le Hir H, Gatfield D, Braun IC, Forler D, Izaurralde E (2001) The protein Mago provides a link between splicing and mRNA localization. EMBO Rep 2: 1119-1124.

Le Hir H, lzaurralde E, Maquat Maquat LE, Moore J (2000) The spliceosome deposits multiple proteins 20-24 nucleotides upstream of mRNA exon-exon junctions. EMBO J 19: 6860-6869.

Lee HC, Choe J, Chi SG, Kim YK (2009) Exon junction complex enhances 31

translation of spliced mRNAs at multiple steps. Biochem Biolphys Res Cummun 384: 334-340.

Lewandowski JP, Sheehan KB Bennett PE, Boswell RE (2010) Mago Nashi, Tsunagi/Y14, and Ranshi form a complex that influences oocyte differentiation in Drosophila melanogaster. Dev Biol 339: 307-319.

Li H, Yuan Z, Vizcay-Barrena G, Yang CY, Liang WQ, Zong J, Wilson ZA, Zhang DB (2011) PERSISTENT TAPETAL CELL1 encodes a PHD-finger protein that is required for tapetal cell death and pollen development in rice. Plant Physiol **156**: 615-630.

Li N, Zhang DS, Liu HS, Yin CS, Li XX, Liang WQ, Yuan Z, Xu B, Chu HW, Wang J, Wen TQ, Huang H, Luo D, Ma H, Zhang DB (2006) The rice tapetum degeneration retardation gene is required for tapetum degradation and anther development. Plant Cell 18: 2999-3014.

Li W, Boswell R, Wood WB (2000) mag-1, a homolog of Drosophila mago nashi, regulates hermaphrodite germ-line sex determination in *Caenorhabditis elegans*. Dev Biol 218: 172-182.

Mamun EA, Alfred S, Cantrill LC, Overall RL, Sutton BG (2006) Effects of chilling on male gametophyte development in rice. Cell Biol Int **30**: 583-591.

Michelle L, Cloutier A, Toutant J, Shkreta L, Thibault P, Durand M, Garneau D, Gendron D, Lapointe E, Couture S, Le Hir H, Klinck R, Elela SA, Prinos P,

Chabot B (2012) Proteins associated with the exon junction complex also control the alternative splicing of apoptotic regulators. Mol Cell Biol 32: 954-967.

Micklem DR, Dasgupta R, Elliott H, Gergely F, Davidson C, Brand A, González-Reyes A, St Johnston D (1997) The mago nashi gene is required for the polarisation of the oocyte and the formation of perpendicular axes in Drosophila. Curr Biol 7: 468-478.

Mohr SE, Dillon ST, Boswell RE (2001) The RNA-binding protein Tsunagi interacts with Mago Nashi to establish polarity and localize oskar mRNA during Drosophila oogenesis. Genes Dev 15: 2886-2899.

Mufarrege EF, Gonzalez DH, Curi GC (2011) Functional interconnections of 32

Arabidopsis exon junction complex proteins and genes at multiple steps of gene expression. J Exp Bot **62**: 5025-5036.

Newmark PA, Boswell RE (1994) The *mago nashi* locus encodes an essential product required for germ plasm assembly in *Drosophila*. Development **120**: 1303-1313.

Newmark PA, Mohr SE, Gong L, Boswell RE (1997) *mago nashi* mediates the posterior follicle cell-to-oocyte signal to organize axis formation in *Drosophila*. Development **124**: 3197-3207.

Nyikó T, Kerényi F, Szabadkai L, Benkovics AH, Major P, Sonkoly B, Mérai Z, Barta E, Niemiec E, Kufel J, Silhavy D (2013) Plant nonsense-mediated mRNA decay is controlled by different autoregulatory circuits and can be induced by an EJC-like complex. Nucleic Acids Res **41**: 6715-6728.

Oliver SN, Van Dongen JT, Alfred SC, Mamun EA, Zhao XC, Saini HS,
Fernandes SF, Blanchard CL, Sutton BG, Geigenberger P, Dennis ES, Dolferus
R (2005) Cold-induced repression of the rice anther-specific cell wall invertase gene *OSINV4* is correlated with sucrose accumulation and pollen sterility. Plant Cell
Environ 28: 1534-1551.

Palacios IM, Gatfield D, St Johnston D, Izaurralde E (2004) An eIF4AIII-containing complex required for mRNA localization and nonsense-mediated mRNA decay. Nature **427**: 753-757.

Park NI, Yeung EC, Muench DG (2009) Mago Nashi is involved in meristem organization, pollen formation, and seed development in *Arabidopsis*. Plant Sci **176**: 461-469.

Parma DH, Bennett PE, Boswell RE (2007) Mago Nashi and Tsunagi/Y14, respectively, regulate *Drosophila* germline stem cell differentiation and oocyte specification. Dev Biol **308**: 507-519.

Ponicsan SL, Kugel JF, Goodrich JA (2010) Genomic gems: SINE RNAs regulate mRNA production. Curr Opin Genet Dev **20**: 149-155.

Qiao F, Zhao KJ (2011) The influence of RNAi targeting of *OsGA20ox2* gene on plant height in rice. Plant Mol Biol Rep **29**: 952-960.

Ramasamy S, Wang H, Quach HN, Sampath K (2006) Zebrafish Staufen1 and Staufen2 are required for the survival and migration of primordial germ cells. Dev Biol **292**: 393-406.

Roignant JY, Treisman JE (2010) Exon junction complex subunits are required to splice *Drosophila* MAP kinase, a large heterochromatic gene. Cell **143**: 238-250.

Shi H, Xu RM (2003) Crystal structure of the *Drosophila* Mago nashi-Y14 complex. Genes Dev 17: 971-976.

Silver DL, Leeds KE, Hwang HW, Miller EE, Pavan WJ (2013) The EJC component *Magoh* regulates proliferation and expansion of neural crest-derived melanocytes. Dev Biol **375**: 172-181.

Tang XR, Wu H, Jia M, Yu XH, He YK (2002) Isolation and expressional analysis of cDNA encoding a dsRNA binding protein homologue OsRBP of rice. J Plant Physiol Mol Biol **28**: 41-45.

Tange TO, Nott A, Moore MJ (2004) The ever-increasing complexities of the exon junction complex. Curr Opin Cell Biol **16**: 279-284.

van der Weele CM, Tsai CW, Wolniak SM (2007) Mago nashi is essential for spermatogenesis in *Marsilea*. Mol Biol Cell **18**: 3711-3722.

Walter M, Chaban C, Schütze K, Batistic O, Weckermann K, Näke C, Blazevic D, Grefen C, Schumacher K, Oecking C, Harter K, Kudla J (2004) Visualization of protein interactions in living plant cells using bimolecular fluorescence complementation. Plant J **40**: 428-438.

Wang K, Peng XJ, Ji YX, Yang PF, Zhu YG, Li SQ (2013) Gene, protein, and network of male sterility in rice. Front Plant Sci 4: 92.

Wang L, Wang Z, Xu Y, Joo SH, Kim SK, Xue Z, Xu Z, Chong K (2009) *OsGSR1* is involved in crosstalk between gibberellins and brassinosteroids in rice. Plant J **57**: 498-510.

Wang Y, Ren Y, Liu X, Jiang L, Chen L, Han X, Jin M, Liu S, Liu F, Lv J, Zhou KN, Su N, Bao YQ, Wan JM (2010) OsRab5a regulates endomembrane organization and storage protein trafficking in rice endosperm cells. Plant J **64**: 812-824.

Xu ML, Jiang JF, Ge L, Xu YY, Chen H, Zhao Y, Bi YR, Wen JQ, Chong K 34 (2005) *FPF1* transgene leads to altered flowering time and root development in rice. Plant Cell Rep **24**: 79-85.

Yang W, Kong Z, Omo-Ikerodah E, Xu W, Li Q, Xue Y (2008) Calcineurin B-like interacting protein kinase OsCIPK23 functions in pollination and drought stress responses in rice (*Oryza sativa* L.). J Genet Genomics **35**: 531-543.

Zhang DB, Wilson ZA (2009) Stamen specification and anther development in rice. Chin Sci Bull **54**: 2342-2353.

Zhang DS, Liang WQ, Yin CS, Zong J, Gu FW, Zhang DB (2010a) OsC6,

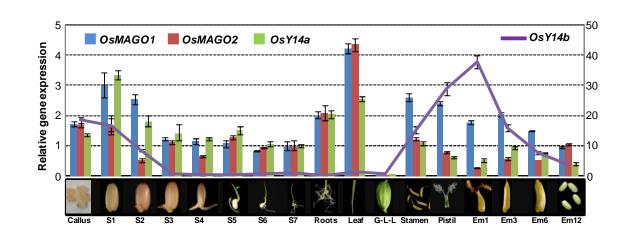
encoding a lipid transfer protein, is required for postmeiotic anther development in rice. Plant Physiol **154**: 149-162.

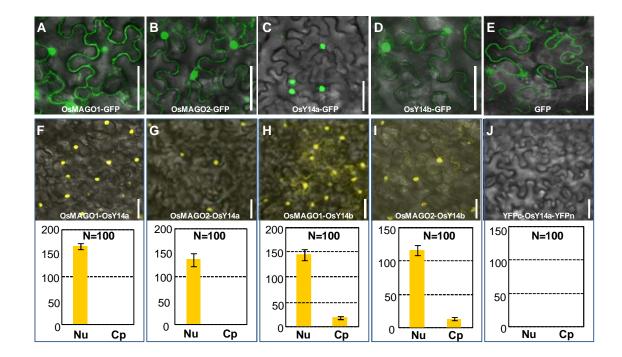
Zhang H, Liang W, Yang X, Luo X, Jiang N, Ma H, Zhang DB (2010b) *Carbon starved anther* encodes a MYB domain protein that regulates sugar partitioning required for rice pollen development. Plant Cell **22**: 672-689.

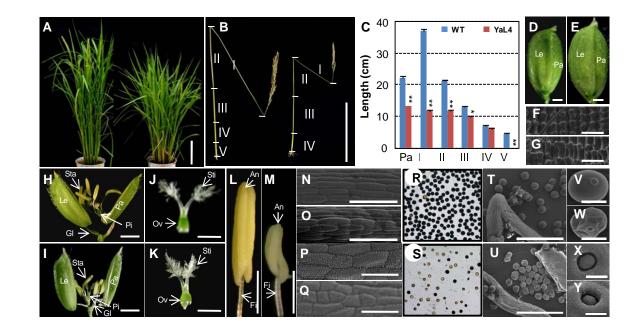
Zhao XF, Nowak NJ, Shows TB, Aplan PD (2000) MAGOH interacts with a novel RNA-binding protein. Genomics **63**: 145-148.

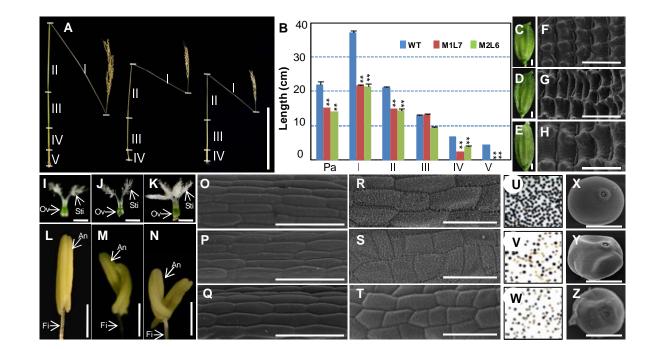
Zhu YY, Nomura T, Xu YH, Zhang YY, Peng Y, Mao BZ, Hanada A, Zhou HC, Wang RX, Li PJ, Zhu XD, Mander LN, Kamiya YJ, Yamaguchi S, He ZH (2006) *ELONGATED UPPERMOST INTERNODE* encodes a cytochrome P450 monooxygenase that epoxidizes gibberellins in a novel deactivation reaction in rice.

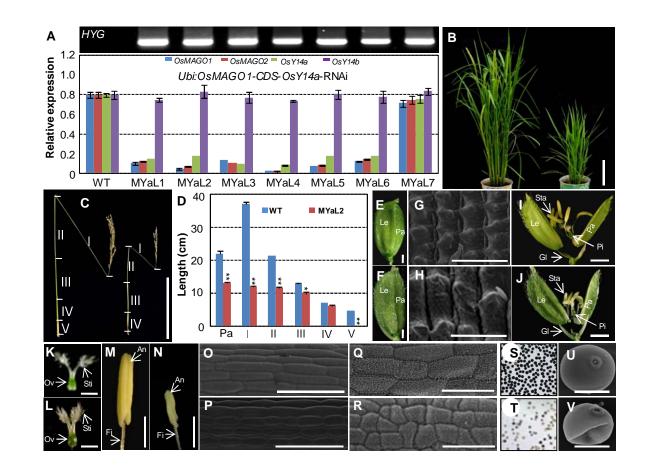
Plant Cell 18: 442-456.

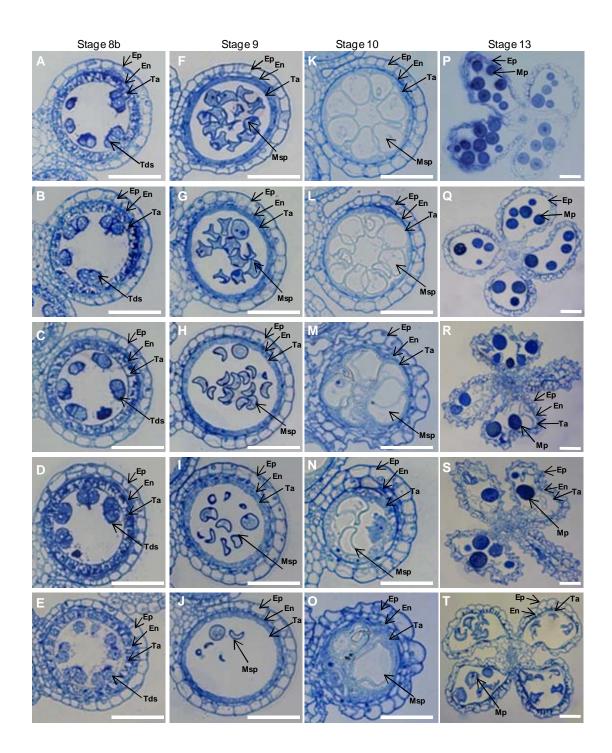












Downloaded from www.plantphysiol.org on May 12, 2014 - Published by www.plant.org Copyright © 2014 American Society of Plant Biologists. All rights reserved.

